Energies **2010**, *3*, 171-193; doi:10.3390/en3020171

OPEN ACCESS

energies

ISSN 1996-1073

www.mdpi.com/journal/energies

Review

Spectrally-Selective Photonic Structures for PV Applications

Marius Peters [1,*], Jan Christoph Goldschmidt [1], Philipp Löper [1], Bernhard Groß [1], Johannes Üpping [2], Frank Dimroth [1], Ralf B. Wehrspohn [2] and Benedikt Bläsi [1]

[1] Fraunhofer Institute for Solar Energy Systems, Heidenhofstraße 2, 79110 Freiburg, Germany; E-Mails: jan.christoph.goldschmidt@ise.fraunhofer.de (J.C.G.); philipp.loeper@ise.fraunhofer.de (P.L.); bernhard.gross@gmail.com (B.G.); frank.dimroth@ise.fraunhofer.de (F.D.); benedikt.blaesi@ise.fraunhofer.de (B.B.)

[2] Martin-Luther-Universität Halle-Wittenberg, Institute of Physics, Heinrich-Damerow-Str.4, 06120 Halle, Germany; E-Mails: johannes.uepping@physik.uni-halle.de (J.Ü.); ralf.wehrspohn@physik.uni-halle.de (R.B.W.)

* Author to whom correspondence should be addressed; E-Mail: marius.peters@ise.fraunhofer.de; Tel.: +49-761-458-851-48; Fax: +49-761-458-892-50.

Received: 24 November 2009 / Accepted: 20 January 2010 / Published: 27 January 2010

Abstract: We review several examples of how spectrally-selective photonic structures may be used to improve solar cell systems. Firstly, we introduce different spectrally-selective structures that are based on interference effects. Examples shown include Rugate filter, edge filter and 3D photonic crystals such as artificial opals. In the second part, we discuss several examples of photovoltaic (PV) concepts that utilize spectral selectivity such as fluorescence collectors, upconversion systems, spectrum splitting concepts and the intermediate reflector concept. The potential of spectrally selective filters in the context of solar cells is discussed.

Keywords: photonic crystals; spectral selectivity; light trapping

1. Introduction

Optical elements are used in many different ways for the task of improving solar cell efficiencies. Examples range from antireflection coatings, *i.e.,* layers deposited directly on the solar cell to reduce front surface reflections [1,2], to lenses or mirrors, devices separated from the cell to concentrate radiation [3,4]. In this paper we focus on a special class of optical elements, namely spectrally

selective filters and how these filters can be used to improve solar cells. The aim of this work is to give an overview of different kinds of applicable filters and of the photovoltaic concepts in which they are used. The defining characteristics of spectrally-selective filters for PV applications are typically:

1. A specific spectral range in which the filter is highly reflective;
2. Another spectral range in which the filter is highly transparent. Frequently, these ranges are close-by, so that an additional requirement is
3. A steep edge between the both ranges.

In most PV concepts, the reflection is used to trap and transport light to the solar cell. A non perfect reflection, therefore, results in a reduction of the light trapping abilities of the system. A non perfect transmission, on the other hand prevents light from entering the solar cell system in the first place and therefore also reduces the light trapping abilities. The combination of all three requirements results in very high demands on the filters in question.

Suitable filter characteristics are provided by interference structures. Light reflected at different places within the structures interferes constructively or destructively, creating the desired high reflectance or transmittance. Several examples of such filters are introduced in the next paragraph. These examples are the Rugate filter, the band stop filter and the opal. Design criteria for these filters are presented and reflection characteristics are shown.

In the subsequent sections, PV applications are discussed that use spectral selectivity. The concepts are distinguished by whether the wavelength of the incident light is changed. The concepts discussed include fluorescent concentrators, upconversion, spectrum splitting by geometrical arrangement or by combination of spectral selectivity and scattering and intermediate reflectors. The list does not make a claim to completeness, as the possibilities with spectrally selective filters are numerous. The aim is, however, to deliver a compendium of the ideas behind spectral selectivity in PV that is adorned with interesting and illustrative examples.

2. Spectrally Selective Interference Filters

In this section several types of interference filters are discussed and advantages and disadvantages of the specific filters are evaluated. Common to all these filters is that the spectral characteristic is created via interference. A periodic arrangement of different materials with different refractive indices typically results in a spectral region in which the reflected or scattered waves superimpose constructively. This phenomenon may be described by the theory of photonic crystals [5]. The spectral region of high reflectance here corresponds to a so-called photonic bandgap. Like the band gap in a semiconductor, the photonic bandgap is a region in the k-space in which certain energy states are forbidden. As the photons may not enter the crystal, they must be reflected. All photonic crystals that possess a photonic bandgap exhibit spectral selectivity in principle. The demand for a high transmission in other spectral regions, however, is sometimes obtained more efficiently, if one diverges from strict periodicity. In general, spectrally selective structures with a convenient characteristic therefore contain periodic and non-periodic aspects.

An important issue in the design of the photonic structure is that the filters have a limited thickness. The limits are set either by production methods of the filters themselves or within the solar cell

concepts. Also the costs of the filters play a considerable role. Real filters will therefore not exceed thicknesses of 10 μm and be much thinner than that in most cases. We have endeavored to include this aspect in the discussion.

In the following, we will concentrate on three examples for filters with convenient characteristics. The first example is the Rugate filter, a structure with a 1D periodic refractive index profile that is additionally modulated. The second example is the edge filter, a structure consisting of two materials that are arranged in alternating layers with aperiodic thicknesses. The third example is the opal, a 3D photonic crystal.

2.1. Rugate Filter

One example for a filter with convenient characteristics is the Rugate filter. The Rugate filter is an advanced version of the Bragg stack. Whereas the Bragg stack consists of two materials and is characterized by a step-function of the refractive index profile, the Rugate filter features a sinusoidal variation of the refractive index. The consequence of this sinusoidal variation is a suppression of harmonic reflections. The Rugate filter has theoretically only a single reflection peak around the design wavelength λ_0. The presence of only a single reflection peak with an adjustable spectral position and width is a valuable characteristic for application on solar cells, as unwanted reflection in the spectral range in which the solar cell absorbs prevents light from entering the solar cell. Losses connected with this process may reduce a positive effect of the filter to zero or even result in an adulterated performance of the solar cell.

The design wavelength for the position of the reflection peak is given by:

$$\lambda_0 = 2 \cdot \bar{n} \cdot \Lambda \tag{1}$$

In this equation, Λ is the period length of one sinus and $\bar{n}$ is the mean refractive index of the filter materials. The mean refractive index is also found in the refractive index profile, which, for a normal Rugate filter, is given by:

$$n(z) = \bar{n} + \Delta n \cdot \sin\left(\frac{2\pi}{\Lambda} \cdot z\right) \tag{2}$$

Here 2 Δn is the maximum refractive index distance. For a typical Rugate filter, the width of the reflection peak is defined by Δn. The higher the contrast, the broader is the reflection peak. This is shown in Figure 1.

A normal Rugate filter still shows sidelobes, *i.e.,* reflections outside the peak region (Figure 2.). To suppress sidelobes, Southwell [6] suggested the use of an envelope function and matching to the adjoined materials. Using these suggestions, the resulting characteristics almost perfectly fit to the demands (Figure 2). It has to be said that an optimization with these steps increases the number of periods needed for a certain reflectance in the peak region.

The characteristics shown in Figure 2 are simulation results. As Figure 2(b) shows, a complete suppression of harmonic reflections is not achieved even with thick Rugate filters.

Optimized Rugate filters are produced with CVD processes (see example [7]). The continuous variation of the refractive indices is achieved by controlling the gas flows. However, to really match

the optimum profile, the control needs to be very accurate and typically the achieved results differ considerably from what is theoretically possible. Especially the suppression of reflections outside the peak region is very hard. Contemporary Rugate filters do not reach the quality of two material assemblies (see next subsection). The control of the width of the reflection peak is limited by the availability of suitable materials. If the absorption needs to be negligible in the visible spectral range, the refractive index ratios are typically in the range of 1.5. Still, the attributes of Rugate filters makes them interesting options for the application on solar cells.

Figure 1. Relative width of the reflection peak of a Rugate filter as a function of the relation of maximum and minimum refractive index of the filter. A relative width of 25% means that, if the design wavelength of the Rugate filter is λ_0 = 800 nm, the width of the peak will be *ca.* 200 nm and the peak will cover a range between λ_- = 700 nm and λ_+ = 900 nm.

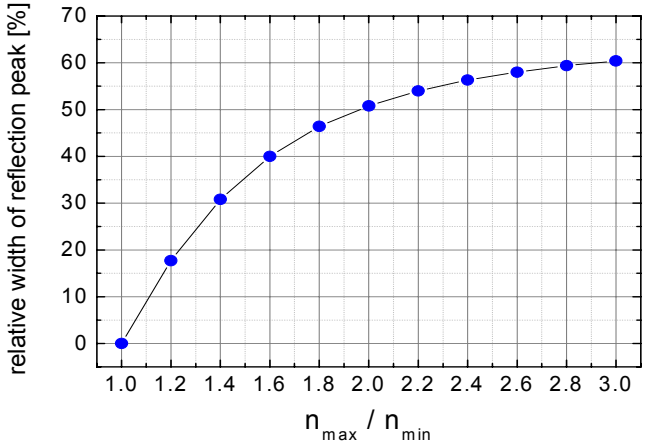

Figure 2. (a) Refractive index profile and (b) reflection characteristics of a normal Rugate filter (light grey) and an optimized Rugate filter (blue). The optimized refractive index profile is enveloped with a Gaussian function and matched to a material with n = 1.5. The related reflection characteristic shows that sidelobes are suppressed, but the first harmonic reflection has not vanished completely. Furthermore, the reflection peak of the optimized filter is narrower than that of the un-optimized case.

(a) (b)

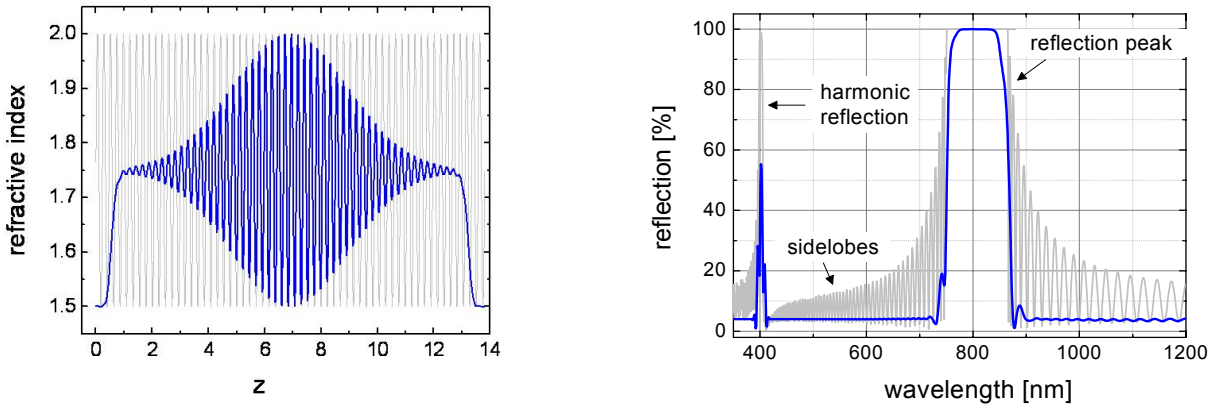

2.2. Edge Filter

Many problems of the Rugate filter can be avoided by using a filter with a simpler assembly. One example for a filter that only consists of two materials but nevertheless shows characteristics that are suitable for PV applications is the edge filter. Whereas the Rugate filter features a modulated periodic function of the refractive index, the edge filter features an a-periodic step function. The edge filter can be obtained from a Bragg stack by varying the thicknesses of the individual layers. In that way, a high reflection is kept in a chosen spectral region, while the a-periodicity is used to suppress reflections outside the peak region. An advantage over the Rugate filter is given by the higher degree of freedom in the design of edge filters. While for the Rugate filter the characteristics for the complete spectrum are defined, for the edge filter only the spectral region of interest needs to be considered.

With aperiodic structures, nearly every desired spectral reflection characteristic can theoretically be realized. In practice, the thickness of the filter limits the characteristics and typically a certain number of layers or a certain filter thickness is chosen and the characteristics are optimized within this presetting. Optimization methods for edge filters can be found in several books on thin film design (example [8]). An interesting method is the needle-optimization algorithm [9].

Figure 3. (a) Distribution of thicknesses for an optimized edge filter and (b) reflection characteristic. The filter was optimized theoretically using an evolutionary algorithm and starting with a Bragg-stack. In the thickness distribution, the red lines give the thicknesses that a Bragg-stack with comparable characteristics would have. The thicknesses of the single layers of the edge filter are distributed around these lines. For the edge filter, therefore, some periodicity remains. The filter was optimized to transmit between λ = 400 nm and λ = 700 nm and to reflect between λ = 700 nm and λ = 1,000 nm. The number of layers used was preset to 76.

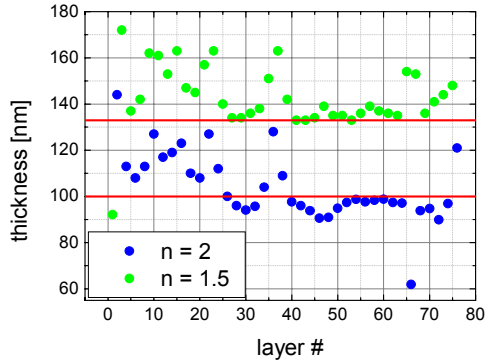

(a)

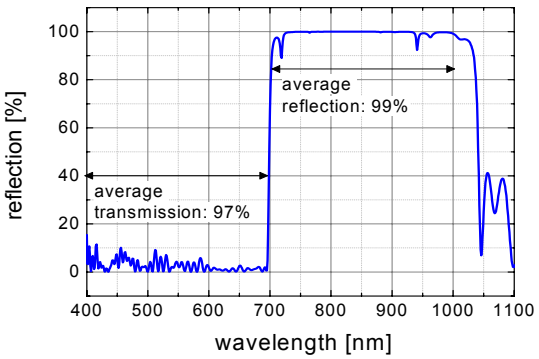

(b)

2.3. Opal

The opal is an example of a 3D photonic crystal. A photonic crystal is an artificial material with a periodic variation of the refractive index in one or more spatial dimensions. The opal consists of spheres that are ordered in an fcc (face centered cubic) lattice. The refractive index of the opal is therefore varied in all three spatial dimensions; therefore it is called a 3D photonic crystal. The Rugate

filter would be an example of a 1D photonic crystal, because the periodicity is formed only in the *z*-direction. The edge filter is not a photonic crystal in the classical sense, because it lacks periodicity.

Characteristic for a photonic crystal is that the dispersion relation of photons within the crystal is displayed in a band diagram. This is an analogy to dielectric crystal, for which the dispersion relation of electrons is displayed in a band diagram. In fact, the whole idea of photonic crystals emerged from this analogy. Within the photonic band structure, photonic band gaps exist; these band gaps are regions in k-space for which no photons can exist within the crystal. For incident photons, a photonic band gap will manifest as a spectral range of high reflection. The opal possesses a photonic band gap for normal incidence [10] in the growth direction of the crystal, causing the formation of a reflection peak. Structure and reflection characteristics of an opal are shown in Figure 4.

Figure 4. (a) Sketch of the opal structure opal and (b) reflection characteristic. Spheres are ordered in a closest package. For this configuration several possibilities exist for the stacking sequence. Mainly two kinds of sequences are distinguished, the sequence ABAB… which corresponds to an hcp (hexagonal closest packed) crystal lattice and ABCABC… which corresponds to the fcc (face centered cubic) crystal lattice. The opal features a photonic band gap which generates a spectrally dependent reflection. The shown characteristic is that of a simulated opal consisting of 22 layers of spheres with n = 1.5 in air. Sphere diameter was set to D = 255 nm.

(a) (b)

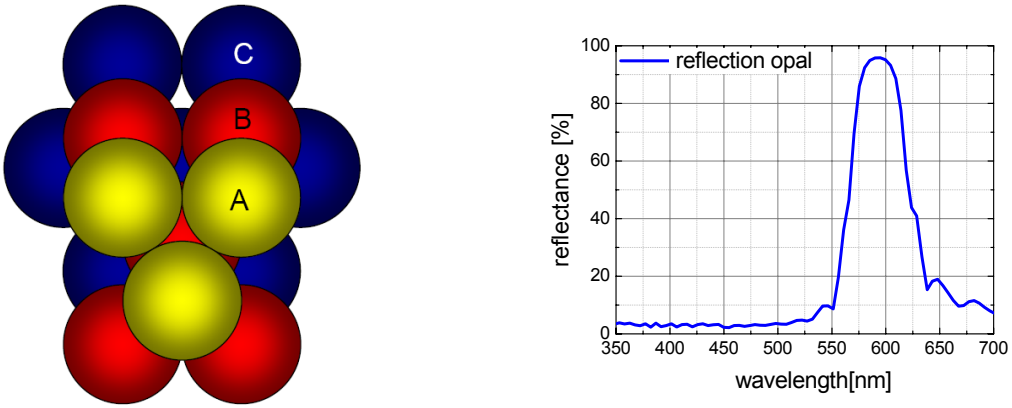

The advantage of opals is that they are formed in a self-organizing process which allows a potentially cheap and fast large scale deposition. However, fabricated opals suffer from several problems. The worst problem is that fabricated opals show much less order than desired. Cracks appear in the opal that are the source of scattering. Most opals therefore show a high reflectance for short wavelengths. Additionally, the disorder has the effect that only a certain amount of sphere layers contribute to the photonic effect. The effective thickness is therefore typically lower than the geometric thickness. Another problem is that harmonic reflections in the opal cannot yet be suppressed. In the Rugate filter, harmonics were suppressed by a grading of the refractive index profile, for the edge filter disorder yielded the desired effect. These strategies are very difficult to apply to the opal. A grading of the refractive index profile is only possible with tremendous experimental effort. Disorder in the opal is initially a source of unwanted scattering. To trigger a certain effect on the spectral

characteristics, disorders would have to be induced intentionally. This procedure would require a lot of additional effort. Despite the mentioned disadvantages, potential applications for the opal exist, especially if 3D photonic properties such as 3D diffractive and spectrally-selective or long pass characteristics are required.

2.4. Angular Dependence

Finally, the angular dependence of spectrally selective filters is briefly discussed. This issue is important because typically filters are designed under the assumption of normal light incidence, but in real-world applications light will impinge on the filter from other directions as well.

In this consideration we assume that the filters are sufficiently periodic, so the angular dependence follows Bragg's condition. This assumption is valid for the Rugate filter. It is valid for the opal for light incident under acute angles ($\alpha < 50°$), and it is valid with constrictions also for the edge filter as the filter is mostly periodic.

The angular dependent characteristic for a periodic filter following Braggs' description is given by:

$$\lambda(\alpha) = \lambda_0 \sqrt{1 - \left(\frac{\sin \alpha}{\overline{n}} \right)^2} \tag{1}$$

In this equation α is the angle of incidence and $\overline{n}$ is the effective refractive index of the filter. The meaning of the equation is that a characteristic of the filter that is located at the wavelength λ_0 for normal incidence shifts to the wavelength $\lambda(\alpha)$ for non-normal incidence. Such characteristics can be, e.g.,, the center position of the reflection peak or the edges. Following this equation, the reflection peak will shift towards lower wavelengths (blue shift) with increasing angles of incidence and the shift will be the stronger, the lower the effective refractive index of the filter is. The blue shift of a Bragg filter is shown in Figure 5. The spectral shift with increasing angles of incidence needs to be considered for the application of filters.

Figure 5. Angular dependent reflection characteristic of a Bragg stack. In the figure, the reflectance of a rugate filter is displayed in dependence of the wavelength and the angle of incidence. The reflection peak of the filter is situated around λ = 1,000 nm and shifts towards the blue for an increasing angle of incidence

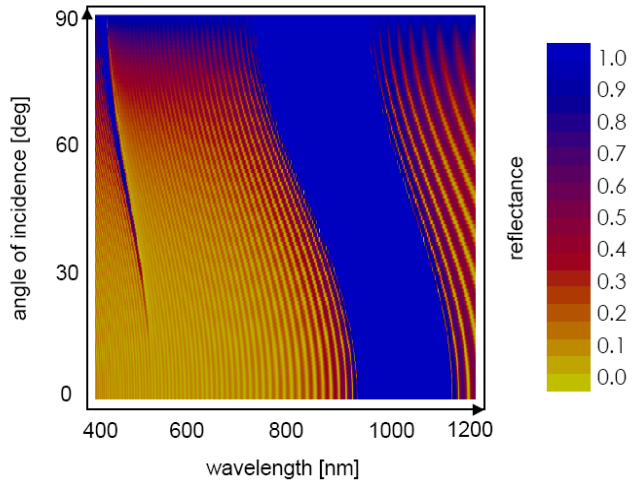

The Bragg description is very general and therefore applies to many interference filters including, to a certain extent, 3D photonic crystals [11,12]. Appearance of the Bragg effect, however, requires periodicity in the plane of incidence. It is therefore possible to deviate from an angular characteristic that is defined by the Bragg effect by using certain non-periodic structures. Such an approach has been suggested for example by Imenes [13].

3. Spectrally Selective Filters for PV Concepts with Luminescent Materials

3.1. Fluorescent Concentrators

The fluorescent concentrator is a device to concentrate diffuse as well as direct radiation. It was developed mainly in the late seventies [14,15] and early eighties [16,17] of the previous century. A fluorescent concentrator is a plate consisting of a synthetic material (e.g., polymethylmethacrylate, PMMA), into which a fluorescent dye is included. The dye absorbs radiation of certain frequencies and later emits radiation that is spectrally shifted towards lower frequencies (Stokes shift). The emitted light is transported via total internal reflection to the edges of the plate, where solar cells are located that convert the arriving radiation into electricity. As the edges typically have a smaller area than the front of the plate, the fluorescent concentrator effects a geometrical concentration of radiation. The idea behind the fluorescent concentrator was to replace expensive solar cells with cheap synthetic materials.

The fluorescent concentrator features several problems that resulted in low efficiencies of the system. Although organic dyes had high quantum efficiencies, these high efficiencies were limited to a narrow spectral range in the visible. Neither for the UV nor for the infrared range could dyes with satisfying quantum efficiencies be found; in the latter case even for fundamental reasons. Other problems are reabsorption caused by an overlap of absorption and emission range of the dye and a limited stability of those dyes sensitive in the infrared. A fundamental loss mechanism is constituted by the transport mechanism directly. It can be assumed that the dye emits light isotropically into every direction. For this reason, a fraction of the emitted light enters the escape cone, *i.e.,* the light is emitted into directions where no total internal reflection occurs. All these problems led to a reduced research interest in the late eighties and in the nineties.

Only recently has the fluorescent concentrator experienced a new burst of interest. One reason for this stimulus is the availability of spectrally matched solar cells that better fit the spectral emission of the dye. Another reason was the development of a concept that aims towards an elimination of the escape cone losses by the application of spectrally selective filters. This idea was proposed by B. Richards in 2004 [18] and by G. Glaeser in 2006 [19]. Currently, several groups are working on fluorescent concentrators again [20-29].

Assuming isotropic emission, the escape cone losses may be estimated as follows: all light emitted into a direction that has a polar component smaller than the critical angle of total internal reflection leaves the concentrator, while all other light is transported without losses. These assumptions are simplifications in several aspects. One aspect is that Fresnel reflections are neglected. This omission is justified because even if light is reflected by Fresnel reflections, the reflectance is generally much lower than 100%. As the light in the escape cone has steep directions, it needs to be reflected many

times to reach the edges, meaning that the amount transported via Fresnel reflections has only a minor effect. Another aspect is that reabsorption effects are neglected. Reabsorption increases the chance for light to enter the loss cone. An estimation of the additional contribution of reabsorption to the escape cone losses is difficult and depends on the geometry on the concentrator. Neglecting reabsorption and assuming perfect reflection for all light for which total internal reflection occurs makes this estimation a lower boundary for the fraction of light in the escape cone:

$$N_{cone} = \frac{\int_0^{2\pi\theta_c}\int_0 \sin\varphi \, d\theta \, d\varphi}{\int_0^{2\pi\pi/2}\int_0 \sin\varphi \, d\theta \, d\varphi} = 1 - \sqrt{\frac{n^2-1}{n^2}} \qquad \text{with} \qquad \theta_c = Arc\sin\left(\frac{1}{n}\right) \tag{2}$$

In this equation θ_c is the critical angle of total internal reflection and n is the refractive index of the synthetic material. A typical value here is n = 1.49, which results in escape cone losses of $N_{cone} \approx 26\%$ [17].

Figure 6. Concept to improve fluorescent concentrators with spectrally selective filters. In the fluorescent concentrator, a dye absorbs light and subsequently emits it with smaller frequency. The light is either emitted into a direction where total internal reflection occurs and is transported to the edges (I), or it is emitted into the escape cone and is, without filter, lost. Typically these escape cone losses cover at least 26% of the emitted light. With a filter, the filter reflects the light in the escape cone and transports it to the edges (II).

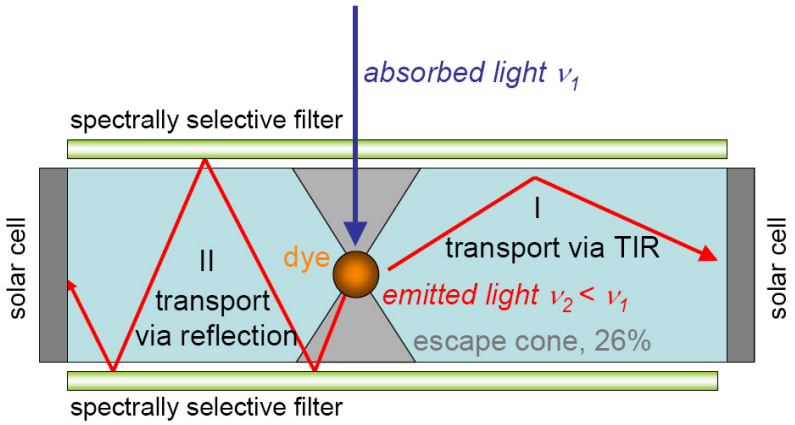

A spectrally selective filter may help to reduce escape cone losses, because the spectral ranges of absorption and emission are separated. It is therefore possible for a filter to reflect the light emitted by a dye but transmit the light absorbed by it. Such a filter would eliminate escape cone losses completely. However, a real filter will show a reduced performance for several reasons. Absorption and emission range of the dye overlap; it is therefore not possible to design the filter in a way that it is transparent for all incident light and reflect all emitted light at the same time. Additionally, the filter will show some reflection in the absorption range of the dye, though these reflections may be reduced if the filter is deposited directly onto the concentrator. Furthermore, the reflectance of the filter will be lower than one in the emission range of the dye so that not all light in the escape cone will be transported to the

edges [30]. A hitherto unsolved problem is the angular dependence of spectrally selective filters. Typically, the reflection peak of such filters is shifted towards smaller wavelengths for increasing angles of incidence. This causes additional losses for all light with non-normal incidence.

These complexities make the demands on filter quality very high. Only a filter with a very low reflectance in the absorption range of the dye, a very high reflection in its emission range and a very steep edge between these two spectral ranges will result in a considerable increase in light guiding efficiency. Specially designed edge filters were used to experimentally examine the effect of spectrally selective filters on the light guiding efficiency of the fluorescent concentrator. In the investigated setup, the edge filter was used with a fluorescent concentrator of quadratic shape, a side length of l = 2.1 cm and a thickness of t = 3 mm. For this setup, the efficiency of a solar cell attached to one side of the concentrator was increased by 19% relative from η = 2.6% to η = 3.1% due to an increase in light guiding efficiency [31].

Figure 7. Characteristics of a fluorescent concentrator and an edge filter optimized for the application on this concentrator. Presented are the reflection characteristics (R) of an optimum and a real filter, as well as the absorption (A) and the photoluminescence (PL) of the dye. The optimum filter would show no reflection in the absorption range of the dye and specular reflection in the PL range. In a real fluorescent concentrator, absorption and PL of the dye overlap, causing reabsorption and prohibiting a complete separation of both ranges. A real filter will reflect some light in the absorption range of the dye and will transmit some light in the PL range.

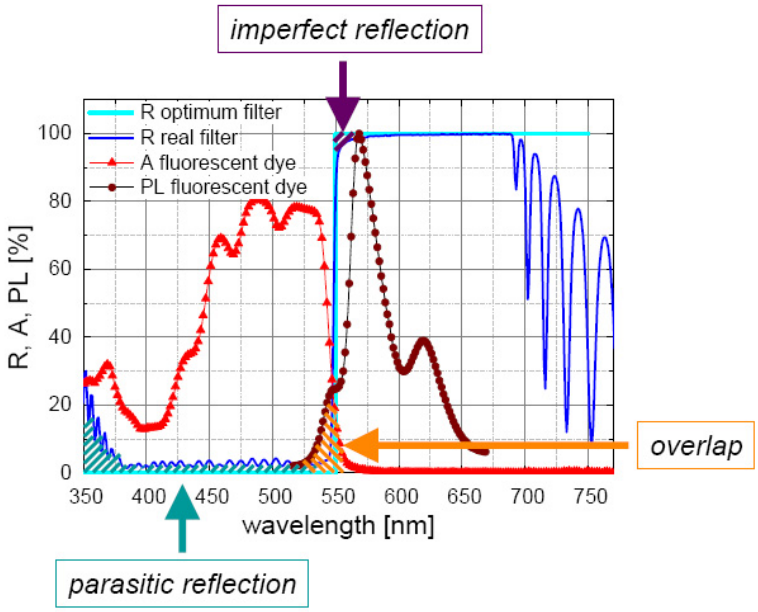

3.2. Upconversion

Photon upconversion is the process of creating one high-energy photon out of at least two low-energy photons. The big advantage of this concept is that it addresses the bottleneck of the low

absorption of long wavelength light in solar cells with nearly no drawbacks. All improvements are real gains, since they come on top of the original performance of the solar cell.

Looking at the example of silicon solar cells, around 20% of the incident solar radiation power is lost because photons with energy below the band-gap are transmitted straight through the device (Figure 8). An ideal upconverter pushes the theoretical efficiency limit from close to 30% up to 40% for a silicon solar cell illuminated by non-concentrated light [32]

Figure 8. Illustration of the fundamental losses in a silicon solar cell, associated with the sub-band-gap (transparency) losses of low-energy photons and the thermalization losses of high-energy photons.

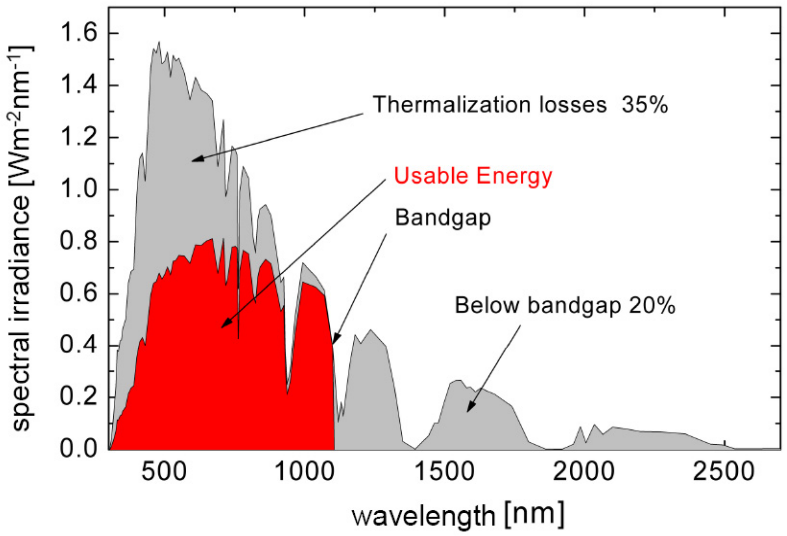

First upconversion systems have been realized experimentally. The highest upconversion efficiencies achieved so far were reported by Richards and Shalav in [33]. They report an external quantum efficiency EQE_{UC} of 3.4% at 1,523 nm laser excitation for a system consisting of a bifacial silicon solar cell and a $NaYF_4:Er^{3+}$ upconverter.

The major problems of common upconverter materials like $NaYF_4:Er^{3+}$ [34] are the narrow absorption range and the high intensity needed for efficient upconversion. Spectrally selective filters are used to overcome these problems.

As an example of how this may be done, an advanced upconversion system shall be discussed. This system is shown in Figure 9. The basic idea behind this system is to use several mechanisms to concentrate light on the upconverter. The first mechanism is *spectral concentration* [35,36]. To achieve spectral concentration, a fluorescent concentrator is used (compare with section "Fluorescent Concentrators"). The task of the fluorescent concentrator is to absorb light in a broad spectral range and emit it in the absorption range of the upconverter. The second mechanism is *geometric concentration*. The upconverting material is placed on small areas between the solar cell and the fluorescent concentrator. It is coupled to the concentrator so that light is able to leave the concentrator only at those places where the upconverting material is situated.

Figure 9: Setup of an advanced upconverter system. The solar cell absorbs photons with energies above the band-gap (ν_1). Photons with less energy are transmitted (ν_2, ν_3). The upconverter transforms especially low energy photons (ν_3) into high energy photons that can be used by the solar cell (ν_1). Photons with energies below the band-gap but above the absorption range of the upconverter (ν_2) are absorbed by a fluorescent concentrator, which emits photons in the absorption range of the upconverter (ν_3). The emitted radiation is guided by total internal reflection and/or photonic structures to the upconverter. As the upconverter does not cover the whole area, a geometric concentration is achieved. Radiation which is emitted from the upconverter towards the fluorescent concentrator is back reflected by a spectrally selective photonic structure [36,37].

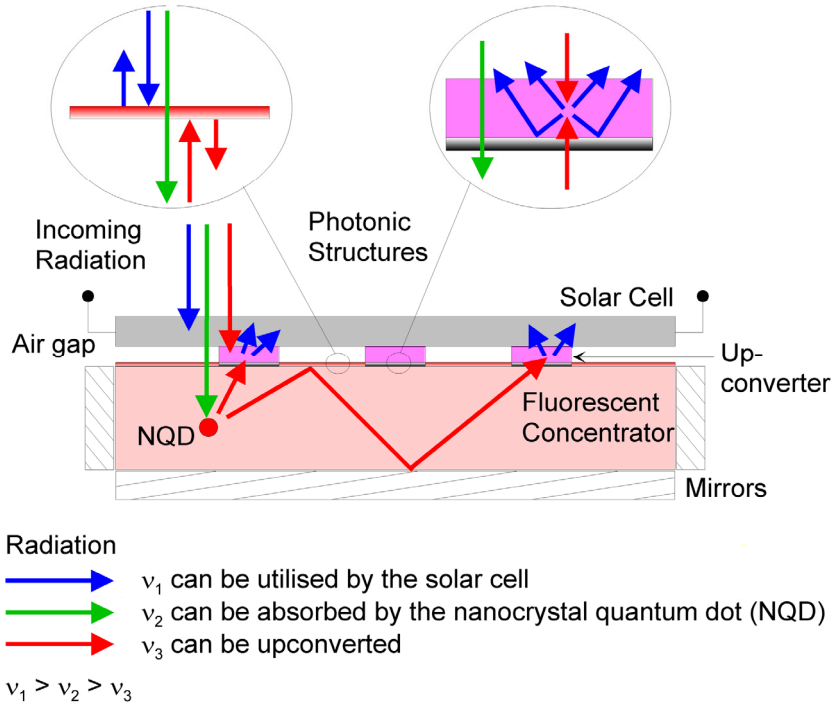

Different spectrally selective filters, selecting different parts of the spectrum, are positioned in different parts of the system for several tasks. First, spectrally selective filters are placed between the upconverter material and the fluorescent concentrator. They are transparent for the light absorbed by the upconverter but reflect the light emitted by the upconverter. In that way no radiation is lost in the direction of the fluorescent concentrator. Secondly, spectrally selective filters may be placed between solar cell and fluorescent concentrator (everywhere where no upconverting material is located) to reduce escape cone losses (see section concerning fluorescent concentrators). Finally, spectrally selective filters may also be placed between upconverter and solar cell to reflect all radiation in the absorption range of the upconverting material, increasing the light intensity in the upconverting material. Positioning luminescent materials inside a cavity is a technique used also in other applications, like e.g.,, laser technologies [38]. Other methods of enhancing the intensity, like e.g., quantum dots [39] are beyond the scope of this work and are only mentioned here for reference.

4. Spectrally Selective Filters for PV Concepts with Spectrum Splitting

4.1. Spectrum Splitting by Geometrical Assembly

A spectral beam splitting architecture does provide an excellent basis for a multi-junction photovoltaic system with virtually ideal band gap combination, thus having the potential to reach very high conversion efficiency. In comparison to monolithically grown multi-junction solar cells, the spectrum splitting is provided by an additional optical element added into the course of the solar beam. On the one hand this optical element is another source for loss mechanisms and increases the complexity of the system, but on the other hand the solar cell material can be selected without constraints to lattice constant and current matching. Due to the missing current limiting constraint, the spectral beam splitting device reveals a higher limiting efficiency [40] and is less sensitive to spectral changes, thus leading to a theoretically higher energy yield. The idea of using a geometrical assembly was first suggested by Jackson. However, the first experimental demonstration was done by Moon *et al.* by applying a 17-layer dichroic reflector stack [41]. More recently, there have been new investigations on spectral beam splitting systems induced by highly accurate thin film deposition technologies currently available [42-45].

A geometrical assembly has been recently fabricated to realize a spectral beam splitting prototype [46]. Figure 10 shows this geometry of the prototype, using two dichroic filters to split the beam into three parts, which are then directed onto three solar cells. The prototype uses a four junction solar cell system (one dual junction solar cell and two single junction solar cells) to convert the partial spectra with high efficiency.

Figure 10. Arrangement of the prototype receiver using the geometry of a 45°-parallelepiped to build a light trapping, spectral beam splitting architecture including three solar cells (one dual junction- and two single junction solar cells) and two beam splitters. The beam splitters are positioned directly in front of the solar cells and are optically connected by a transparent layer of silicone.

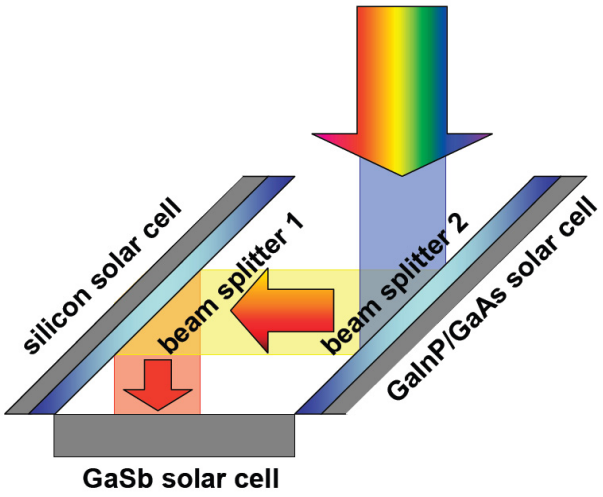

Two spectral beam splitters with short pass characteristics were used to split the sunlight. Figure 11 shows the transmission characteristics of dichroic filter 1 and 2. The transmission band of filter 1 transmits the sunlight between 380 and 850 nm, whereas between 850 and 1,800 nm the light is reflected. Dichroic filter 2 transmits in a wider wavelength range (380–1,080 nm) and therefore reflects just between 1,080–1,800 nm. As shown, edge filters for photovoltaic applications need to provide broadband characteristics, which causes thick filter stacks of up to several hundred layers.

The edge filters were simulated and deposited using TiO_2 as high refractive index material and SiO_2 as low index counterpart. The filter structures are similar to the one shown in Figure 3. The filters used for this investigation consisted of 220 layers. Such a dielectric stack presents a complex, but close to ideal example of an advanced optical element for photovoltaic applications.

Figure 11. Optical transmission of spectral beam splitter (a) and (b) as used in the prototype with edge wavelength at 850 (1,080) nm. The blue line shows the simulated characteristics as is the case in a system set up with 45° incidence angle. The red line shows the measured transmissions of the fabricated beam splitters with back reflections of the filter substrate glass while not connected to the solar cells. The measured characteristic is close to the simulated one (thin dotted black line), showing virtually ideal characteristics. The spectrally weighted transmissions between 380 and 850 (1,080) nm is 96.4% (95.5%) while the reflectance between 850 (1,080) and 1,800 nm is 98.1% (97.2%) Reproduction with permission from B. Gross, the figure appears in [46].

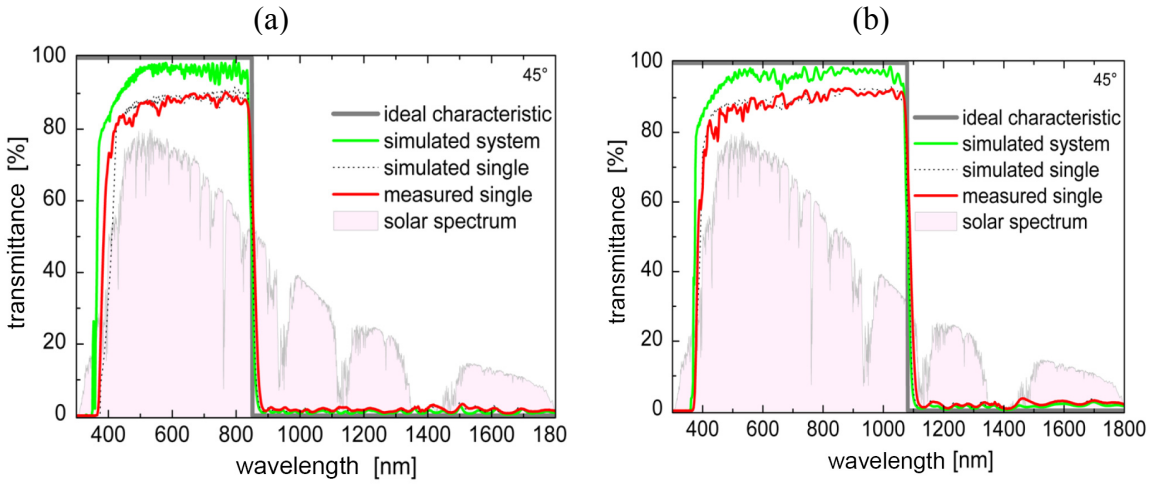

The system described in this section was realized and reached efficiencies of more than 30% under one sun illumination [46].

4.2. Spectrum Splitting with Diffuse Light Trap

The idea of a diffuse light trap is to scatter the internal light so that it sooner or later reaches every point inside the trap. In that way every solar cell inside the light trap is illuminated with the same spectrum. An optimum filter needs to transmit only the part of the spectrum that is most beneficial for a certain solar cell and reflect all other light. The optimum optical characteristics of the filters, the

ranges of high transmittance and high reflectance, of the filters depend sensitively on the specific solar cell system. An optimization with the aim of maximizing the system efficiency has to be carried out for each concept independently. A typical starting point is to chose a band pass filter, *i.e.,* a filter that is perfectly transparent in a certain spectral range and reflects perfectly everywhere else.

Now, the optical efficiency of the trap shall be estimated. Independent of the exact construction of the light trap, the photon flux into and out of the light trap will be equal under equilibrium conditions. Let us now consider the situation for light of a certain wavelength. The flux into the cell is the light entering the trap through the entrance aperture A_{ent}. The flux out of the light trap is made up of several contributions:

- The light absorbed by the solar cell for which the light is intended. This contribution depends on the solar cell area A_{c1} and the reflection of the filter in front of it R_{c1}.
- The light absorbed by any other solar cell. This contribution depends on the solar cell area A_{c2} and the reflection of the filter in front of it R_{c2}.
- The light absorbed by the walls of the light trap. This contribution depends on the area not covered by solar cells A_t and the absorption of the trap Abs_t.
- The light leaving the trap through the entrance aperture A_{ent}

In a simple approach, the following assumptions were made: the light inside the light trap is perfectly diffuse. The trap includes three solar cells that each cover the same area ($A_{c1} = A_{c2}$), each corresponding to 10% of the trap surface so that the chance of being hit by a photon is 10% for each solar cell. The chance for a photon of being accepted by the different solar cells is defined by an effective transmission $T_{c1} = 1–R_{c1}$ (for the intended solar cell) and an effective reflection R_{c2} (for the solar cells the photon is not intended to reach). To simplify things, both values T_{c1} and R_{c2} were varied simultaneously and it was assumed that they take the same value. In the variation shown in Figure 13, a negligible size of the entrance aperture was assumed and the absorption at the trap walls was varied. Several more variations have been carried out which are not shown here. Already from these simple estimations, several conclusions about the properties of the light trap can be drawn:

- The entrance aperture should be small compared to the area covered by the intended solar cell. The relation of aperture area A_{ent} to cell area A_{c1} defines the minimum loss.
- The quality of the filter should be as high as possible but some imperfections are acceptable. A reduction in filter quality of 1% will roughly reduce the optical efficiency by 1% per solar cell for which the light is not intended.
- The area in the light trap covered by solar cells should not be too small. Otherwise, wall absorption will become more and more important. Even in the moderate setup considered with 30% wall covering, wall absorption of 1% decreases the optical efficiency by *ca.* 6%. If the wall covering is halved, the reduction already increases to *ca.* 15% per percent absorption.

Several examples for diffuse light traps have been proposed. One example is the photovoltaic cavity converter (PVCC), which has been investigated by several groups [47-49]. This device consists of a spherical light trap with a white colored interior, similar to an Ulbricht sphere. Solar cells are attached to the sphere interior. Light is concentrated onto a small entrance aperture. The solar cells are equipped with spectrally selective pass filters, which are transparent in the spectral range intended for the solar

cell. The light is distributed uniformly inside the sphere so that every solar cell is illuminated with the same spectrum. Another diffuse light trap has been described by Goetzberger [50]. This light trap was designed as a planar concentrator made of a material with refractive index n. Light scattering in combination with total internal reflection results in an increased light intensity inside the light trap. Solar cells are attached to the plate and are equipped with spectrally selective pass filters, transparent in the intended absorption range of the cell. As diffuse light traps suffer from losses through entrance aperture and wall absorption, this concept has not yet become popular.

Figure 12. Dependence of the optical efficiency of the diffuse light trap on the filter quality and the absorption at the walls. Calculated was the fraction of photons accepted by the intended solar cell. For a perfect filter characteristic (T_{c1} = R_{c2} = 1) and no wall absorption, all photons arrive at the intended solar cell. With increasing wall absorption and decreasing filter quality the optical efficiency drops. Losses caused by the aperture area are neglected.

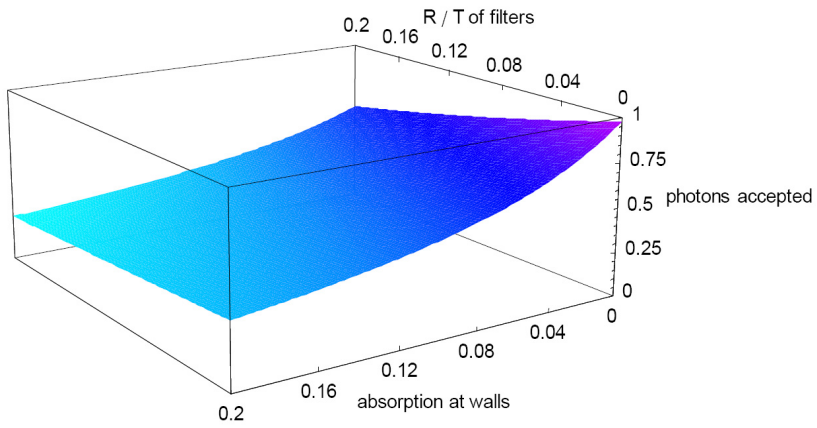

Figure 13. Sketch of the light traps proposed by (a) Ortabasi and (b) Goetzberger. The main differences between these concepts is that the light bulb is filled with air, while the light trap by Goetzberger ideally has a body made of a high index material to increase the internal intensity.

(a) (b)

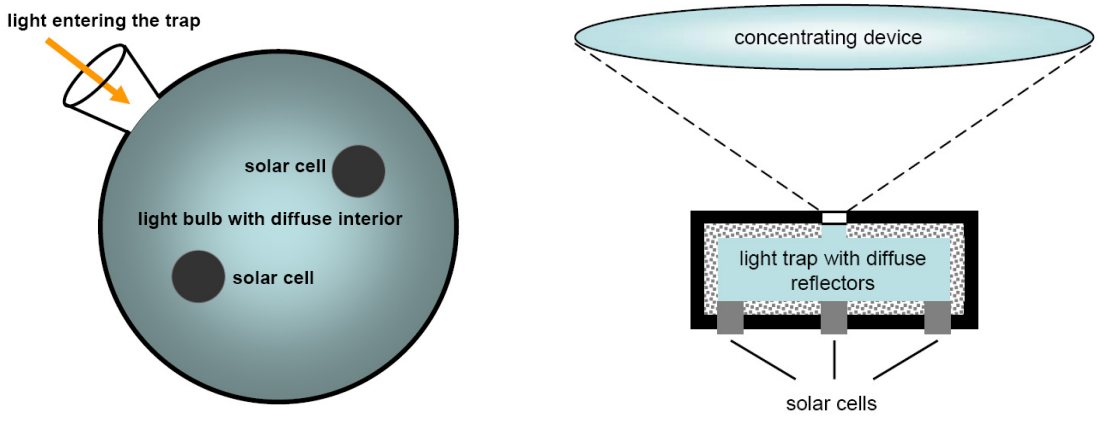

4.3. Intermediate Reflectors

For several reasons it is beneficial to stack different solar cells on top of each other. The different solar cells use different parts of the solar spectrum, and the combination results in an increased efficiency of the stacked system compared to what a single solar cell can achieve [51]. Stacked solar cells, however, face several problems of their own, one of which being that the current of all cells must be matched because the cell with the lowest current limits the current of the entire system [52]. Spectrally selective filters can be used for this purpose, as shall be discussed here for the example of the micromorph tandem cell.

The micromorph tandem cell combines a top cell made of hydrogenated amorphous silicon (a-Si:H) and a bottom cell made of microcrystalline silicon (μc-Si). The a-Si:H solar cell is a thin film solar cell that can be produced cheaply but shows a relatively low efficiency. The micromorph tandem cell concept combines this low cost thin film approach with the highly efficient tandem cell concept. A sketch of the concept is shown in Figure 14.

Figure 14. Schematic sketch of the micromorph tandem cell concept. The top cell is deposited directly on a textured zinc oxide front glass (front glass + TCO). The texturing introduces a roughness which is essential for light trapping in the thin solar amorphous silicon solar cell. Between the two solar cells, the intermediate reflector is placed, increasing the number of photons absorbed by the top cell. The bottom cell is followed by another TCO contact and a metallic back reflector. The bottom cell's thickness is *ca.* 2 μm, while the top cell's thickness is limited to 0.15−0.3 μm.

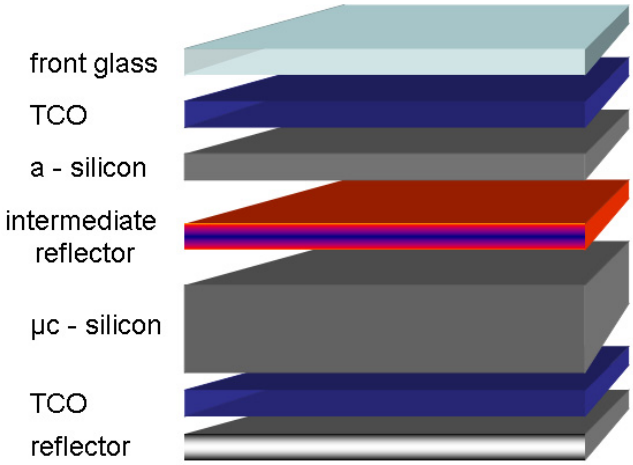

The a-Si:H top cell has the larger electrical band gap, therefore the voltage produced by this cell is higher than the voltage from the μc-Si bottom cell. Also the current generated by both cells is different, as the top cell generates a lower current. The properties of the cells are characterized by their external quantum efficiencies (EQE), shown in Figure 15.

In the spectral region where the EQEs of top- and bottom cell overlap, a spectrally selective intermediate reflector can be used to reflect photons into the top cell, increasing the quantum efficiency and the photon current. [53-55]. The characteristic of this reflector is that photons in the spectral overlap between λ = 550 nm and λ = 700 nm are reflected, while photons with higher

wavelengths are transmitted. This concept has convenient aspects for the solar cell concept as well as for the filters used.

Figure 15. External quantum efficiencies of the two junctions of a micromorph tandem cell [53]. High energy photons are nearly completely absorbed in the top a-Si:H cell, low energy photons are transmitted to the bottom µc-Si cell and are absorbed there. For wavelengths above λ = 550 nm, the EQE of the top cell is limited by the low absorption coefficient.

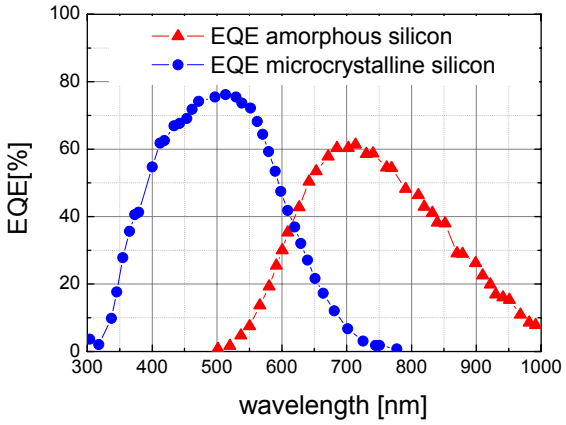

For the solar cells, the use of the intermediate reflector is beneficial for two reasons:

- The current mismatch between the two cells is decreased. Typically, the top cell limits the system current. The intermediate reflector increases the top cell current.
- The voltage of the top cell is higher. Therefore every photon used by the top cell instead of the bottom cell converts a larger fraction of its energy into electricity.

The optical filter required for this concept has to meet several conditions:

1. In order not to lose photons, the filter needs to be transparent for all photons that are used more beneficially by the bottom cell than by the top cell.
2. The filter has to reflect exactly the number of photons that is required for current matching. The filter therefore does not need a certain very high reflection, but the reflection characteristic needs to be matched to the solar spectrum and the quantum efficiency [56].
3. As the tandem is connected in series, the filter needs to be sufficiently electrically conductive. This demand is the most special one, as typical optical filters do not need this property.

A structure which meets all of these demands is the inverted opal [57]. The lowest photonic bandgap of the opal in the Γ-L direction provides a spectrally selective reflection. As the lowest photonic bandgap was chosen, no further reflections for higher wavelengths must be expected. By choosing the photonic bandgap according to the spectral overlap of the quantum efficiencies of top and bottom solar cell, the first two demands are met. To meet the third demand, the inverted opal can be fabricated from a conductive material. One of these materials is aluminium doped ZnO [58], but other materials like SiC are also possible. For such a system, a relative increase of 10% was predicted.

5. Summary

In this work we summarized several aspects of how solar cell systems may be improved by spectrally selective optical elements. We started with a discussion of several spectrally selective filters. Three examples were chosen here that frequently are used in the context of solar cells. The first example is the optimized Rugate filter, the second example is the edge filter and the third example is the artificial opal. All of these filters have several advantages and disadvantages that make them especially interesting for different PV applications. We discussed design criteria for such filters and showed typical reflection characteristics. After that we discussed several PV concepts that use the aforementioned filters. The first example is the fluorescent concentrator. Here spectral selectivity is used to reduce losses from the most important loss mechanism, the escape cone of total internal reflection. By the application of an edge filter, the current of a solar cell attached to the side of the concentrator was increased by 20%, corresponding to an equally high capture of lost photons. The second example is up-conversion. Spectrally selective filters here are used to guide the desired part of the spectrum onto the up-converting material and to support the concentration of this non-linear process. The third example discussed is spectrum splitting by geometrical arrangement. Here spectrally selective filters are used to distribute different parts of the solar spectrum onto solar cells with different band gaps that utilize the considered part of the spectrum most efficiently. In this example, the distribution is achieved via a geometrical arrangement. A prototype reached an efficiency of more than 30% under non-concentrated illumination. The fourth example considers a distribution of the solar spectrum by scattering. The filters here are used to reflect all light that is not intended for a certain solar cell. The solar cells are integrated into a light trap with diffuse interior. Beside high demands on the filter, the diffuse reflectance of the light trap and the size of the entrance aperture here play an important role. In the fifth and final example, intermediate reflectors in tandem solar cells are discussed. This concept has very special demands on the spectrally selective filter. As the filter is positioned directly between the different solar cells, it needs to be electrically conductive. By applying the filter, more photons are absorbed in the front cell and less in the bottom cell, which allows for current matching between these cells.

The presented selection of examples is not complete. Concepts that have not been discussed are e.g., photonic crystal back reflectors in solar cells [59] or heat management by selectively reflecting the infrared part of the spectrum [60]. However, already the presented examples demonstrate the wide range of possibilities existing for the application of spectrally selective photonic structures for PV applications. It also demonstrates the potential to improve solar cells by the use of optical and photonic concepts.

Acknowledgments

This work has been supported by the DFG-Project “Nanosun” and the BMBF project “Nanovolt”. The authors thank all cooperation partners of Nanosun and Nanovolt, and especially Tim Rist and Elisabeth Schäffer from Fraunhofer ISE for their support

References and Notes

1. Green, M.A. *High Efficiency Silicon Solar Cells*; Trans Tech Publications: Aedermannsdorf, Switzerland, 1987; pp. 181-183.
2. Wang, A.; Zhao, J.; Green, M.A. 24% efficient silicon solar cells. *Appl. Phys. Lett.* **1990**, *57*, 602-604.
3. Gordon, J.M. Concentrator Optics. In *Concentrator Photovoltaics*; Luque, A., Andreev, A. Eds.; Springer Verlag: Berlin, Germany, 2007; pp. 113-133.
4. Burgess, E.L.; Pritchard, D.A. Performance of a one kilowatt concentrator photovoltaic array utilizing active cooling. In *Proceedings of the 13th Photovoltaic Specialists Conference*, New York, NY, USA, June 1978; pp. 1121-1124.
5. Joannopoulos, J.D.; Meade, R.D.; Winn, J.N. *Photonic Crystals Molding the Flow of Light*. Princeton University Press: Princeton, NJ, USA, 1995; pp. 8-45.
6. Southwell, W.H.; Hall, R.L. Rugate filter sidelobe suppression using quintic and Rugated quintic matching layers. *Appl. Opt.* **1988**, *28*, 2949-2951.
7. Lim, S.; Ryu, J.; Wager, J.; Plant, T. Rugate filters grown by plasma-enhanced chemical vapor deposition. *Thin Solid Films* **1994**, *245*, 141-145.
8. Macleod, H.A. *Thin-Film Optical Filters*, 3rd ed.; Institute of Physics Publishing: Philadelphia, PA, USA, 2001; pp. 11-32.
9. Sullivan, B.T.; Dobrowolski, J.A. Implementation of a numerical needle method for thin-film design. *Appl. Opt.* **1996**, *35*, 5484-5492.
10. Sözüer, H.S.; Haus, J.W.; Inguva, R. Photonic bands: Convergence problems with the plane-wave method. *Phys. Rev. B: Condens. Matter Mater. Phys.* **1992**, *45*, 13962-13972.
11. Gajiev, G.M.; Golubev, V.G.; Kurdyukov, D.A.; Medvedev, A.V.; Pevtsov, A.B.; Sel'kin, A.V.; Travnikov, V.V. Bragg reflection spectroscopy of opal-like photonic crystals. *Phys. Rev. B: Condens. Matter Mater. Phys.* **2005**, *72*, 205115:1-205115:9.
12. Peters, M.; Goldschmidt, J.C.; Kirchartz, T.; Bläsi, B. The photonic light trap – improved light traping in solar cells by angularly selective filters. *Sol. Energy Mater. Sol. Cells* **2009**, *93*, 1721-1727.
13. Imenes, A.G.; Buie, D.; McKenzie, D. The design of broadband, wide-angle interference filters for solar concentrating systems. *Sol. Energy Mater. Sol. Cells* **2006**, *90*, 1579-1606.
14. Weber, W.H.; Lambe, J. Luminescent greenhouse collector for solar radiation. *Appl. Opt*. **1976**, *15*, 2299-2300.
15. Goetzberger, A.; Greubel, W. Solar energy conversion with fluorescent collectors. *Appl. Phys.* **1977**, 14, 123-139.
16. Wittwer, V.; Heidler, K.; Zastrow, A.; Gotzberger, A. Theory of fluorescent planar concentrators and experimental results, *J. Lumin.* **1981**, *24/25*, 873-876.
17. Zastrow, A. *Physikalische Analyse der Energieverlustmechanismen in Fluoreszenz-konzentratoren*; Dissertation, Ùniversität Freiburg: Freiburg, Germany, 1981.
18. Richards, B.S.; Shalav, A.; Corkish, R.P. A low escape-cone loss luminescent solar concentrator. In *Proceedings of the 19th European Photovoltaic Solar Energy Conference*, Paris, France, June, 2004; pp. 113-116.

19. Glaeser, G.C.; Rau, U. Collection and conversion properties of photovoltaic fluorescent concentrators with photonic band stop filters. In *Photonics for Solar Energy Systems (Proceedings Volume)*; Gombert, A., Ed.; SPIE: Bellingham, WA, USA, 2006.
20. Luque, A.; Martı´, A.; Cuadra, L.; Algora, C.; Wahnon, P.; Sala, G.; Benitez, P.; Bett, A.W.; Gombert, A.; Andreev, V.M.; Jassaud, C.; Van Roosmalen, J.A.M.; Alonso, J.; Raüber, A.; Strobel, G.; Stolz, W.; Bitnar, B.; Stanley, C.; Conesa, J.C.; Van Sark, W.; Barnham, K.; Danz, R.; Meyer, T.; Luque-Heredia, I.; Kenny, R.; Christofides, C. Fullspectrum: A new PV wave making more efficient use of the solar spectrum. In *Proceedings of the 19th European Photovoltaic Solar Energy Conference*, Paris, France, June 2004; pp. 336-339.
21. Van Roosmalen, J.A.M. Molecular-based concepts in PV towards full spectrum utilization. *Semiconductors* **2004**, *38*, 970-975.
22. Goldschmidt, J.C.; Peters, M.; Hermle, M.; Glunz, S.W. Characterizing the light guiding of fluorescent concentrators. *J. Appl. Phys.* **2009**, *105*, 114911:1-114911:9.
23. Richards, B.S.; Shalav, A. The role of polymers in the luminescence conversion of sunlight for enhanced solar cell performance. *Synth. Met.* **2005**, *154*, 61-64.
24. Rau, U.; Einsele, F.; Glaeser, G.C. Efficiency limits of photovoltaic fluorescent collectors, *Appl. Phys. Lett.* **2005**, *87*, 171101:1-171101:3.
25. Glaeser, G.C.; Rau, U. Collection and conversion properties of photovoltaic fluorescent concentrators with photonic band Stopp filters. In *Proceedings of SPIE 2006*, San Jose, CA, USA, January, 2006; doi: 10.1117/12.669638.
26. Goldschmidt, J.C.; Peters, M.; Löper, P.; Schultz, O.; Dimroth, F.; Glunz, S.W.; Gombert, A.; Willeke, G. Advanced fluorescent concentrator system design. In *Proceedings of the 22nd European Photovoltaic Solar Energy Conference*, Milan, Italy, September 2007; pp. 608-612.
27. Danos, L.; Kittidachachan, P.; Meyer, T.J.J.; Greef, R.; Markvart, T. Characterisation of fluorescent collectors based on solid, liquid and langmuir blodget (LB) films. In *Proceedings of the 21st European Photovoltaic Solar Energy Conference*, Dresden, Germany, September 2006; pp. 443-446.
28. Debije, M.G.; Broer, D.J.; Bastiaansen, C.W.M. Effect of dye alignment on the output of a luminescent solar concentrator. In *Proceedings of the 22nd European Photovoltaic Solar Energy Conference*, Milan, Italy, September 2007; pp. 87-89.
29. Slooff, L.H.; Budel, T.; Burgers, A.; Bakker, N.; Büchtemann, A.; Danz, R.; Meyer, T.; Meyer, A. The luminescent concentrator: stability issues. In *Proceedings of the 22nd European Photovoltaic Solar Energy Conference*, Milan, Italy, September 2007; pp. 584-588.
30. Peters, M.; Goldschmidt, J.C.; Löper, P.; Bläsi, B.; Gombert, A. The effect of photonic structures on the light guiding efficiency of fluorescent concentrators. *J. Appl. Phys.* **2009**, *105*, 014909:1-014909:10.
31. Goldschmidt, J.C.; Peters, M.; Bösch, A.; Helmers, H.; Dimroth, F.; Glunz, S.W.; Willeke, G. Increasing the efficiency of fluorescent concentrator systems. *Sol. Energy Mater. Sol. Cells* **2009**, *93*, 176-182.
32. Trupke, T.; Shalav, A.; Richards, B.S.; Würfel, P.; Green, M.A. Efficiency enhancement of solar cells by luminescent up-conversion of sunlight. *Sol. Energy Mater. Sol. Cells* **2006**, *90*, 3327-3338.

33. Richards, B.S.; Shalav, A. Enhancing the near-infrared spectral response of silicon optoelectronic devices via up-conversion. *IEEE Trans. Electr. Devices* **2007**, *54*, 2679-2684.
34. Krämer, K.W.; Biner, D.; Frei, G.; Güdel, H.U.; Hehlen, M.P.; Lüthi, S.R. Hexagonal sodium yttrium fluoride based green and blue emitting upconversion phosphors. *Chem. Mater.* **2004**, *16*, 1244-1251.
35. Strümpel, C.; McCann, M.; del Cañizo, C.; Tobías, I.; Fath, P. Erbium-doped up-converters on silicon solar cells: Assessments of potentials. In *Proceedings of the 20th EUPVSEC*, Barcelona, Spain, June 2005.
36. Goldschmidt, J.C.; Löper, P.; Fischer, S.; Janz, S.; Peters, M.; Glunz, S.W.; Willeke, G.; Lifshitz, E.; Krämer, K.; Biner, D. Advanced upconverter systems with spectral and geometric concentration for high upconversion efficiencies. In *Proceedings of IUMRS-ICEM08*, Sydney, Australia, July 2008, pp. 307-311.
37. Goldschmidt, J.C.; Löper, P.; Peters, M. Bundesrepublik Deutschland, Fraunhofer-Gesellschaft zur Förderung der angewandten Forschung e.V. Deutsches Patent 102007,045,546, 2009.
38. Bhawalkar, J.D.; He, G.S.; Park, C.K.; Zhao, C.F.; Ruland, G.; Prasdan, P.N. Efficient two-photon pumped green upconverted cavity lasing in a new dye. *Opt. Commun.* **1996**, *124*, 33-37.
39. Lifshitz, E.; Brumer, M.; Kigel, A.; Sashchiuk, A.; Bashouti, M.; Sirota, M.; Galun, E.; Burshtein, Z.; Le Quang, A.Q.; Ledoux-Rak, I.; Zyss, J. Air-stable PbSe/PbS and PbSe/$PbSe_xS_{1-x}$ core-shell nanocrystals quantum dots and their applications. *J. Phys. Chem. B* **2006**, *110*, 25356-25365.
40. Shockley, W.; Queisser, H.J. Detailed balance limit of efficiency of p-n junction solar cells. *J. Appl. Phys.* **1961**, *32*, 510-519.
41. Moon, R.L.; James, L.W.; Vander Plas, H.A.; Yep, T.O.; Antypas, G.A. Multigap solar cell requirements and the performance of AlGaAs and Si cells in concentrated sunlight. In *Proceedings of the 13th IEEE Photovoltaic Specialists Conference*, New York, NY, USA, 1978; pp. 859-867.
42. Barnett, A.; Kirkpatrick, D.; Honsberg, C.; Moore, D.; Wanlass M.; Emery, K.; Schwartz, R; Carlson, D.; Bowden, S.; Aiken, D. Very high efficiency solar cell modules. *Prog. Photovoltaics: Res. Appl.* **2009**, *17*, 75-83.
43. Fraas, L.M.; Avery, J.E.; Huang, H.X.; Minkin, L.; Shifman, E. Demonstration of a 33% efficient cassegrainian solar module. In *Proceedings of the 4th World Conference on Photovoltaic Energy Conversion*, Hawaii, HI, USA, May 2006; pp. 679-682.
44. Vincenzi, D.; Busato, A.; Stefancich M.; Martinelli, G. Concentrating PV system based on spectral separation of solar radiation. *Physica. Status Solidi: A* **2009**, *206*, 375-378.
45. Bielawny, A.; Miclea, P.T.; Rhein, A.; Wehrspohn, R.B.; Van Riesen. S.; Glunz, S. Dispersive elements for spectrum splitting in solar cell applications, In *Proceedings of SPIE 2006*, San Jose, CA, USA, January 2006; p. 619704.
46. Groß, B.; Peharz, G.; Siefer, G.; Peters, M.; Gandy T. Four-junction spectral beam splitting photovoltaic receiver with high optical efficiency. *Prog. Photovoltaics: Res. Appl.* **2009**, (in press).
47. Ortabasi, U. First experiences with a multi-bandgap photovoltaic cavity converter (PVCC) module for ultimate solar-to-electricity conversion efficiency. In *Proceedings of the 19th European Photovoltaic Solar Energy Conference*, Paris, France, June 2004; pp. 2256-2560.

48. Imenes, A.G.; Mills, D.R. Spectral beam splitting technology for increased conversion efficiency in solar concentrating systems: a review. *Sol. Energy Mater. Sol. Cells* **2004**, *84*, 19-69.
49. Minano, J.C.; Luque, A.; Tobias, I. Light-confining cavities for photovoltaic applications based on the angular-spatial limitation of the escaping beam. *Appl. Opt.* **1992**, *31*, 3114-3122.
50. Goetzberger, A.; Goldschmidt, J.C.; Peters, M.; Löper, P. Light trapping, a new approach to spectrum splitting. *Sol. Energy Mater. Sol. Cells* **2008**, *92*, 1570-1578.
51. De Vos, A. Detailed balance limit of the efficiency of tandem solar cells. *J. Phys. D: Appl. Phys.* **1980**, *12*, 839-846.
52. Repmann, T. Investigations on the current matching of highly efficient tandem solar cells based on amorphous and microcrystalline silicon. In *Proceedings of 3rd World Conference on Photovoltaic Energy Conversion*, Osaka, Japan, May 2003; pp. 1843-1846.
53. Wieder, S.; Rech, B.; Roschek, T.; Müller, J.; Wagner. H. In *Proceedings of the E-PVSEC*, Glasgow, UK, May 2000; p. 561.
54. Steinhauser, J.; Shah, A.; Ballif, C.; Domin´e, D.; Bailat, J. Micromorph solar cell optimization using a ZnO layers as intermediate reflector. In *Conference Record of the 2006 IEEE 4th World Conference on Photovoltaic Energy Conversion*, Hawaii, HI, USA, May 2006; pp. 1465-1468.
55. Dominé, D.; Steinhauser, J.; Feitknecht, L.; Shah, A.; Ballif, C. Effect of ZnO layer as intermediate reflector in micromorph solar cells. In *Proceedings of the 20th EU Photovoltaic Solar Energy Conference*, Barcelona, Spain, June 2005; pp. 1600-1603.
56. Bielawny, A.; Üpping, J.; Wehrspohn, R. Spectral properties of intermediate reflectors in micromorph tandem cells. *Sol. Energy Mater. Sol. Cells* **2009**, *93*, 1909-1912.
57. Yamamoto, K.; Nakajima, A.; Yoshimi, M.; Sawada, T.; Fukuda, S.; Suezaki, T.; Ichikawa, M.; Koi, Y.; Goto, M.; Meguro, T.; Matsuda, T.; Sasaki, T.; Tawada, Y. High efficiency thin film silicon hybrid cell and module with newly developed innovative interlayer. In *Conference Record of the 2006 IEEE 4th World Conference on Photovoltaic Energy Conversion*, Hawaii, HI, USA, May 2006; pp. 1489–1492.
58. Bielawny, A.; Üpping, J.; Miclea, P.T.; Wehrspohn, R.B.; Rockstuhl, C.; Lederer, F.; Peters, M.; Steidl, L.; Zentel, R.; Lee, S.; Knez, M.; Lambertz, A.; Carius, R. 3d photonic crystal intermediate reflector for micromorph thin-film tandem solar cell. *Phys. Stat. Sol. B* **2008**, *205*, 2796-2810.
59. Shvarts, M.Z.; Chosta, O.I.; Kochnev, I.V; Lantratov, V.M.; Andreev, V.M. Radiation resistant AlGaAs/GaAs concentrator solar cells with internal Bragg reflector, *Sol. Energy Mater. Sol. Cells* **2001**, *68*, 105-122.
60. Krisl, M.E.; Sanchez, J.; Sachs, I.M. Thin film coatings for improved coverglass thermal characteristics. In *Proceedings of the 18th IEEE Photovoltaic Specialists Conference*, Las Vegas, NV, USA, October 1985; pp. 692-696.